

# Physics of Spontaneous Calcium Oscillations in Cardiac Cells and Their Entrainment

Ohad Cohen\* and Samuel A. Safran

Department of Chemical and Biological Physics, Weizmann Institute of Science, Rehovot 76100, Israel

(Received 17 September 2018; revised manuscript received 20 February 2019; published 15 May 2019)

Mechanical contraction in muscle cells requires Ca to allow myosin binding to actin. Beating cardiomyocytes contain internal Ca stores whose cytoplasmic concentration oscillates. Our theory explains observed single channel dynamics as well as cellular oscillations in spontaneously beating cardiomyocytes. The Ca dependence of channel activity responsible for Ca release includes positive feedback with a delayed response. We use this to predict a dynamical equation for global calcium oscillations with only a few physically relevant parameters. The theory accounts for the observed entrainment of beating to an oscillatory electric or mechanical field.

DOI: 10.1103/PhysRevLett.122.198101

Cardiac contraction is a process driven by calcium oscillations, coupled to the mechanical, actomyosin contraction of the heart cell [1] [see Fig. 1(a)], and has a typical timescale of  $\sim 1$  Hz [2–4]. This is achieved by numerous types of ionic pumps and channels embedded in the cellular membrane and in an organelle called the sarcoplasmic reticulum (SR) [5–8], which permeates the entire cell volume and serves as an internal  $\text{Ca}^{2+}$  reservoir. Calcium dynamics are schematically shown in Fig. 1. In muscle cells,  $\text{Ca}^{2+}$  is usually maintained at low concentrations in the cytoplasm and high concentrations in the SR. Spontaneous activation of a the cardiac cell is usually induced by fluctuations or changes in ion channel and pump activity, which causes an influx of  $\text{Ca}^{2+}$  ions into the cytoplasm. The  $\text{Ca}^{2+}$  then activates SR embedded ryanodine receptor (RyR) channels which further release the  $\text{Ca}^{2+}$  stored in the SR into the cytoplasm in a process known as calcium-induced calcium release (CICR) [5]. After a certain amount of  $\text{Ca}^{2+}$  is released, RyR channels close and ionic pumps restore the cytoplasmic  $\text{Ca}^{2+}$  concentration to its baseline value [5]. An important observation is that RyR channels show an adaptive response to changes in  $\text{Ca}^{2+}$  concentration [9]. Experiments demonstrated that the opening probability of RyR channels sharply increases in response to a rapid increase in  $\text{Ca}^{2+}$  concentration from  $\sim 0.1$  to  $\sim 10 \mu\text{M}$ , and shows exponential relaxation to a steady-state value with a typical timescale of  $\sim 100$  ms [9]. This observation motivates and is explained by our theory for local, single channel dynamics, which we then extend to explain global, spontaneous calcium oscillations in the entire cell.

The  $\text{Ca}^{2+}$  released by the channels diffuses to the vicinity of the contractile units (sarcomeres) in these cells and allows myosin binding to actin and hence contraction [10]. It is worth noting that mechanical oscillations of actomyosin at a much faster timescale have been observed in other *in vivo* [11–14] and reconstituted systems [15]. However, in

cardiomyocytes  $\text{Ca}^{2+}$  oscillations persist even when contractility is nearly abolished by introducing blebbistatin [16], indicating that  $\text{Ca}^{2+}$  is indeed the driving force behind contraction in muscle cells.

Previous models of calcium dynamics [17–24] focus on the short time, molecular details of the coupled,

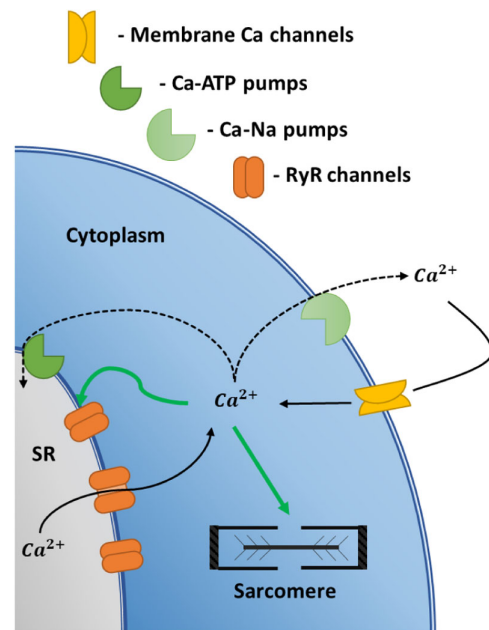


FIG. 1. Schematic representation of calcium dynamics in cardiac cells. A  $\text{Ca}^{2+}$  influx from the environment to the cytoplasm occurs due to fluctuations in calcium channels and pump activity. This causes a release of stored  $\text{Ca}^{2+}$  from the sarcoplasmic reticulum (SR) through SR embedded RyR channels. The increase in cytoplasmic  $\text{Ca}^{2+}$  concentration facilitates both contraction of actomyosin in sarcomeres and further opening of RyR channels (green arrows). Eventually, RyR channels close, and various ion pumps and channels restore  $\text{Ca}^{2+}$  to its original concentration (dashed lines), and the cycle begins again.

multicomponent kinetic processes that underlie  $\text{Ca}^{2+}$  oscillations. A key feature of many of those models is the slow regulatory process that causes a time delay in the response of calcium channels to changes in cytoplasmic  $\text{Ca}^{2+}$  [17–20]. Here, we show that such a time-delayed response is crucial to obtain spontaneous oscillations. We first focus on single channel dynamics and feedback which we then extend to a predictive, mesoscale theoretical approach for global  $\text{Ca}^{2+}$  oscillations in the cell. We begin with a model of the RyR channel kinetics and their sensitivity to the  $\text{Ca}^{2+}$  kinetics via the CICR mechanism, which is consistent with the *in vitro* observations of changes in the channel opening probability dynamics. This is then used, together with a kinetic rate equation for the global  $\text{Ca}^{2+}$  concentration, to analytically predict a transition from a stable steady state to spontaneous oscillations at frequencies much smaller than the channel opening or closing kinetic rates.

We start by describing the dynamics of the average RyR channel probability  $P(t)$  [ $1 - P(t)$ ] to be open [closed], and begin with the naive assumption that the rate constants for opening and closing ( $R^\pm$ ) react to the *instantaneous*  $\text{Ca}^{2+}$  concentration [ $C(t)$ ]:

$$\dot{P} = R^+(C) - [R^+(C) + R^-(C)]P. \quad (1)$$

The  $\text{Ca}^{2+}$  dynamics are described by a simple minimal kinetic equation:

$$\dot{C} = JP - KC. \quad (2)$$

Thus, the system has only two time-dependent degrees of freedom  $P$  and  $C$ . In general, both the opening and closing rates of the channel  $R^\pm(C)$  can be calcium dependent, and are on the order of  $\sim 100$  Hz [19,25]. The theoretical treatment is the same even if the closing rate is independent of calcium [see Supplemental Material (SM) [26]]. Calcium induces RyR channel opening for low (micromolar) concentrations, and channel closing for high (millimolar) concentrations. [5,6,18,27]. Equation (2) relates the change in intracellular calcium concentration to the opening probability multiplied by the maximum  $\text{Ca}^{2+}$  current  $J(C) > 0$  from the SR to the cytoplasm. We start with the case where the current is independent of the cytoplasmic  $\text{Ca}^{2+}$  [i.e.,  $J(C) \approx J$ ] and show later on that nonlinear terms (which can come from calcium dependence of the flux) are crucial to stabilize the amplitude of oscillations. The calcium loss term proportional to  $K$  accounts (in a lumped manner) for numerous mechanisms such as SR  $\text{Ca}^{2+}$ -ATPase activity, membrane bound  $\text{Na}^+$ - $\text{Ca}^{2+}$  pumps, and mitochondrial  $\text{Ca}^{2+}$  uniports. All of these reduce the cytoplasmic  $\text{Ca}^{2+}$  concentration [5]. The steady-state solution of Eqs. (1) and (2) is given by  $\bar{P} = R^+(\bar{C})/R$ , with  $R = [R^+(\bar{C}) + R^-(\bar{C})]$  the combined rate at steady

state, and  $\bar{C} = J\bar{P}/K$  the cytoplasmic, steady-state  $\text{Ca}^{2+}$  concentration. We next examine small perturbations about this steady state by defining the scaled variables  $c = (C - \bar{C})/\bar{C}$  and  $p = (P - \bar{P})/\bar{P}$ , and expanding Eqs. (1) and (2) about the steady state to get the scaled equation (see SM for derivation [26]):

$$\dot{p} = R[-p(t) + \alpha c(t)], \quad (3)$$

$$\dot{c} = K[p(t) - c(t)], \quad (4)$$

where  $\alpha$  is a measure of the linearized dependence of the rate equations on the  $\text{Ca}^{2+}$  concentration, and we take the realistic limit of a channel which is mostly closed [9] (i.e.,  $\bar{P} \ll 1$ ; see SM for full derivation [26]). The rescaled channel dynamics is faster than the rescaled calcium reclamation ( $R \gg K$ ), which implies that  $\text{Ca}^{2+}$  is slowly varying while RyR channels are in a state of quasisteady state. The experiments in Ref. [9] show that when calcium is sharply increased from low ( $\sim 0.1 \mu\text{M}$ ) to high ( $\sim 1$  or  $10 \mu\text{M}$ ) concentrations,  $p(t)$  initially overshoots and then slowly relaxes to its steady-state values with a typical timescale of  $\sim 100$  msec (see Fig. 2 of Ref. [9]). The authors termed this an “adaptive response” of the RyR channel which cannot be resolved by steady-state experiments where the RyR opening probability is measured only at long times [9]. The use of the naive approximation Eq. (3) cannot explain these dynamical experiments on single channels (see SM [26]) and Eq. (3) can only explain RyR dynamics for a very slow increase of ( $\sim 10$  sec [9]) or fixed  $\text{Ca}^{2+}$  concentrations. In addition, Eq. (3) predicts relaxational dynamics and not oscillations for the global concentration. This is seen in the realistic limit of  $R \gg K$ , where we approximately write  $p(t) \approx \alpha c(t)$ , which when used in Eq. (4) yields:

$$\dot{c} = -K(1 - \alpha)c, \quad (5)$$

yielding strictly relaxation dynamics. Thus, the adiabatic dependence of the channel opening probability on the instantaneous  $\text{Ca}^{2+}$  concentration alone in Eq. (3) is insufficient also to explain spontaneous oscillations.

The observed “adaptive” response to a sharp increase in  $\text{Ca}^{2+}$  can be accounted for by including the dependence of channel dynamics not only on the adiabatic  $\text{Ca}^{2+}$  concentration but also on the rate of change  $\dot{c}(t)$  of this concentration. This rate dependence can originate, for example, from a relatively long, delayed, regulatory response that controls the rate at which calcium binds to the channel [17,18,20]. We model such an effect in a generic manner by supplementing Eq. (3) with a history-dependent adaptive response, using a memory function with a rate  $H$  termed the adaption rate:

$$\dot{p} = R \left( -p(t) + \alpha c(t) + \beta H \int_{-\infty}^t \dot{c}(t') e^{-H(t-t')} dt' \right), \quad (6)$$

with  $\beta$  a proportionality constant. This predicts channel dynamics consistent with the experiments of Ref. [9]. A sharp increase in calcium is equivalent to  $\dot{c}(t) \sim \Delta c \delta(t)$ , which yields for our model a rapid increase in  $p(t)$  at short times, followed by an exponential decrease to steady state. For fixed or very slowly increased  $\text{Ca}^{2+}$ , the second term in Eq. (6) is negligible and we reproduce the results of Eq. (3) via the adiabatic term proportional to  $\alpha$ . The added term  $\sim \beta$  introduces an effective time delay in the RyR channel response, where the channel takes time to adapt to the new conditions imposed by changes in  $\text{Ca}^{2+}$ . This is analogous to viscoelastic materials where the propagation of deformation throughout a body is retarded by friction at the microscopic level [28–30]. The channel response thus lags behind the calcium variations, introducing an effective memory to the system. To continue, we consider again the realistic limit of  $R \gg 1$  Hz. The adaptation dynamics ( $\sim 10$  Hz) is still faster than the 1 Hz calcium oscillations, which allows us to treat the integral in Eq. (6) as sharply peaked around  $t = t'$  (since  $H \gg 1$  Hz). We therefore expand the relatively slowly varying calcium  $c(t')$ , for small values of  $t - t' > 0$ , to get

$$p(t) \approx \alpha c(t) + \beta H \dot{c}(t) \int_{-\infty}^t e^{-H(t-t')} dt' + \beta H \ddot{c}(t) \int_{-\infty}^t e^{-H(t-t')} (t' - t) dt' + \dots \quad (7)$$

Integrating Eq. (7), we find  $p(t) \approx [\alpha c(t) + \beta \dot{c}(t) - (\beta/H) \ddot{c}(t)]$ , where we kept the leading terms in  $H^{-1}$ . When introduced into Eq. (4) we get after some rearrangement (see SM [26]):

$$\ddot{c} + \epsilon \dot{c} + \Omega_c^2 c = 0, \quad (8)$$

with  $\epsilon = H[1/(\beta K) - 1]$  and  $\Omega_c = \sqrt{(1-\alpha)H/\beta}$ , which is indeed slower than channel dynamics ( $\Omega_c \ll R$ ). Here  $\epsilon$  is an effective dissipation term which is a net result of pumps that remove Ca from the cytoplasm (positive) and RyR channels (negative) that transfer Ca from the SR to the cytoplasm. For  $\epsilon > 0$ , small perturbations slowly relax back to steady state ( $c = 0$ ). However, when the channel feedback exceeds an activation threshold  $K\beta > 1$  (with higher order corrections derived in the SM [26]), which leads to an ever-increasing cytoplasmic  $\text{Ca}^{2+}$  concentration. Inclusion of the adaptive term in Eq. (6) is therefore crucial to shift the system from a stable steady state to spontaneous oscillations. As is common in such negative dissipation systems [31], this increase is saturated due to the presence of higher-order, nonlinear dissipative terms to avoid divergence. These terms can arise from several different

microscopic effects, such as expansion of the rates  $R^\pm$  to higher order than linear in the  $\text{Ca}^{2+}$  concentration or the  $\text{Ca}^{2+}$  concentration dependence of the ionic flux through the channel (see SM [26]). As is usual [31], here we include such a term, proportional to  $\Gamma$ , phenomenologically:

$$\ddot{c} + \epsilon \dot{c} + \Gamma c^2 \dot{c} + \Omega_c^2 c = 0. \quad (9)$$

Equation (9), derived using separation of timescales of single channel dynamics and global calcium kinetics, is the well-known Van der Pol equation for a nonlinear oscillator [32]. For  $\epsilon < 0$ ,  $|\epsilon| \ll 1$ , the system shows spontaneous oscillations with an approximate frequency  $\Omega_c$  and amplitude  $a_c \approx 2\sqrt{|\epsilon|/\Gamma}$ . Since cells in experiments switch stochastically between spontaneous beating and quiescence [33,34], we expect those cells to lie close to criticality ( $|\epsilon| \ll 1$ ). In this regime the frequency scales like  $\Omega_c \sim \sqrt{(1-\alpha)KH}$ , which can indeed be of the order of  $\sim 1$  Hz. The adaptive, time-delayed response of the RyR channel results in an effective ‘‘inertia’’ (which similarly expresses the time-delayed response of CICR activation) and ‘‘negative dissipation,’’ which are crucial to generate spontaneous  $\text{Ca}^{2+}$  oscillations as observed in cardiac cells [2–4,34,35]. One way to show this is by slowing the adaptation rate  $H$ , to the extent that RyR channels cannot adjust to calcium modulations. This can be achieved by decreasing MgATP concentrations in the cell, which was shown, in single channel experiments, to increase the adaptation time to  $\sim 1.5$  sec [9]. We predict that a significant change in the Mg concentration in cardiomyocytes may cause spontaneously beating cells to switch to quiescence.

In the SM [26] we compare the approximate, single effective Eq. (9) for calcium oscillations with the full dynamics of Eqs. (4) and (6). The amplitudes and frequencies predicted by the intuitive, approximate, Eq. (9), match those of the numerical solution of the full dynamics given by Eqs. (4) and (6) (see SM [26]). Inclusion of additional nonlinearities in the ‘‘dissipation’’ (terms proportional to  $\sim \dot{c}$ ) and ‘‘stiffness’’ (terms proportional to  $\sim c$ ) can modify the waveform and frequency of the oscillations compared to the sinusoidal-like predictions of Eq. (9). Those then become more similar to observed oscillations, with a sharp increase in concentration followed by a slow quiescence (see SM [26]).

Next, we consider a beating cell in the presence of an external pacing force. Calcium oscillations can be paced either electrically [36–39] or mechanically [33,34]. For electrical pacing, the cell is subject to an external electrical field which causes voltage sensitive ion channels on the cell membrane to open, inducing an influx of ions to the cytoplasm [40]. For mechanical stimulation, the cell is subject to an oscillating mechanical force which can couple to the cell membrane (or the SR), through integrin adhesions [41]. The tension applied to the cell membrane (or the SR

membrane) can modulate the activity of mechanosensitive protein complexes which, in turn, modifies the kinetics of calcium release from SR [42]. Effectively, the tension translates into a flux of  $\text{Ca}^{2+}$  into the cytoplasm (either from the environment or from the SR).

To account for such direct pacing we add an external, oscillating pacing force  $f(t) = a_p \Omega_c^2 \cos(\Omega_p t)$  on the right-hand side of Eq. (9), where  $a_p$  and  $\Omega_p$  are, respectively, the amplitude and frequency of the pacing (the  $\Omega_c^2$  factor is introduced so that  $a_p$  is dimensionless). To proceed, we follow Refs. [35,43] and examine the solution for the case where the cell oscillations are entrained to that of the applied force (i.e., the cell oscillates with the frequency of the external force):

$$c(t) = a \cos[\Omega_p t + \phi_c(t)], \quad (10)$$

where  $a$  is the steady-state amplitude of the resulting  $\text{Ca}^{2+}$  oscillations and  $\phi_c(t)$  is the phase relative to the external pacing force. Using the methods of averaging [32,43], we find that entrainment by the external force implies that the phase must attain a constant value at long times (see SM [26]) [44]. In this limit ( $\phi_c \rightarrow \text{const}$ ) one can derive the condition for entrained, steady-state oscillations:

$$Q = \left| \frac{a_p}{a(a_p)} \frac{1}{(1 - \omega_p^2)} \right| \geq 1, \quad (11)$$

where we define the dimensionless frequency ratio  $\omega_p = \Omega_p/\Omega_c$ . Generally speaking, the amplitude of  $\text{Ca}^{2+}$  oscillations  $a(a_p)$  is a function of the amplitude of the pacing forces  $a_p$ . In the limit of weak pacing force  $a_p \ll 1$ , the net  $\text{Ca}^{2+}$  oscillation magnitude can be approximated by its spontaneous value in the absence of pacing  $a(a_p) \approx a_c$ . If the difference between the frequencies of the cell and the external force is too large, or if the amplitude of the external force is much weaker than the amplitude of spontaneous  $\text{Ca}^{2+}$  oscillations, the cell will not synchronize to the external force. Since the onset of full synchronization begins when  $Q = 1$ , for small pacing force, we can analytically calculate a curve that gives the locus of the onset of entrainment as a function of the amplitude and frequency of the applied force:

$$\frac{a_p}{a_c} = |1 - \omega_p^2|. \quad (12)$$

Figure 2 shows the analytical prediction for the onset of entrainment as a solid black line, where above the curve the cellular oscillations are entrained to those of the external force and below the cell beats with a combination of the spontaneous frequency and that of the pacing force. The analytical approximation of Eq. (12) is compared in Fig. 2 to the numerically estimated onset of synchronization [calculated from Eq. (9) with an added pacing term] by

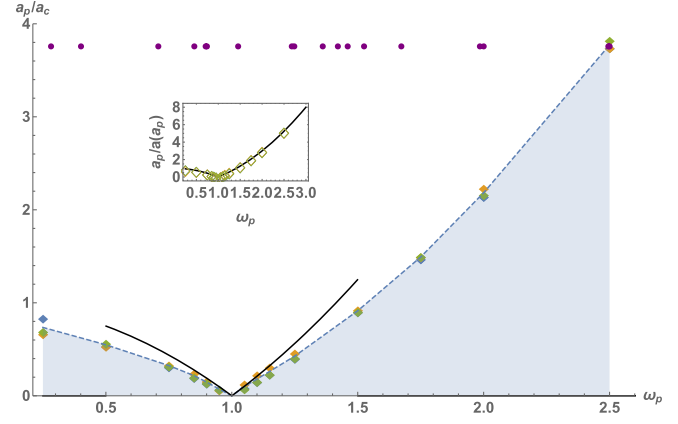


FIG. 2. Analytical and numerical calculations, and experimental data, showing the onset of synchronization as a function of amplitude ( $a_p/a_c$ ) and frequency ( $\omega_p = \Omega_p/\Omega_c$ ) ratios. Parameters were chosen at the edge of the physical range to explore the most dramatic changes. The black line is the analytical approximation of Eq. (12) (valid when  $\omega_p \approx 1$ ). The blue dashed line connects the averages of the numerically calculated values (a guide to the eye). Below the curve (shaded area), the beating dynamics contains both the cell and the probe frequencies, while above the curve, cells are entrained to the external force (i.e., they beat with frequency  $\Omega_p$ ). Color legend: (blue)  $\epsilon = -0.1, \Gamma = 5$ , (orange)  $\epsilon = -0.5, \Gamma = 1.4$ , (green)  $\epsilon = -0.02, \Gamma = 10$ . Purple circles show the reproduced data from Ref. [34], showing entrainment for a fixed amplitude ratio estimated by the transition from entrained to nonentrained beating at  $\omega_p \approx 2.5$ . Inset: Same numerical results plotted for the amplitudes ratio  $a_p/a(a_p)$ , where  $a(a_p)$  is evaluated directly from the numerical solution. Black curve given by Eq. (12) where the amplitude of oscillations  $a$  is not approximated by  $a_c$ , but rather extracted from the numerical calculations.

fixing  $\omega_p$  and slowly increasing  $a_p$  until entrainment is observed. Regardless of the values chosen for the parameters  $\epsilon$  and  $\Gamma$ , the estimated transition to entrainment occurs for the same amplitude ratio. This suggests that entrainment is only weakly dependent on the individual microscopic model parameters ( $R^+, R^-, \alpha, \beta, J, K$ ) but is strongly dependent on the emergent mesoscopic parameters ( $a_c, \Omega_c$ ) scaled to those of the pacing force ( $a_p, \Omega_p$ ). In this manner we obtain a universal curve in a plot of the amplitude ratio  $a_p/a_c$  vs the frequency ratio  $\omega_p = \Omega_p/\Omega_c$ . The analytical estimate of Eq. (12) (the dashed curve in Fig. 2) matches the numerics as long as the difference between the spontaneous and external force frequencies is small ( $\omega_p \approx 1$ ), with larger deviations for larger frequency differences. When the cell amplitude  $a(a_p)$  is estimated directly from the numerical solutions of Eq. (9) and the ratio  $a_p/a(a_p)$  is plotted instead, the numerics match the curve for all values of rescaled probe frequency  $\omega_p$  (Fig. 2, inset). This suggests that the  $\text{Ca}^{2+}$  amplitude scales in a way that indeed maintains a fixed value of  $Q \approx 1$  for the transition to entrainment. Note that a complex model for

synchronization of  $\text{Ca}^{2+}$  oscillations in hepatocytes (solved numerically) in Ref. [23] results in a similar plot for the onset of entrainment. When our intuitive method is applied (see SM [26]) to that model for the same parameter values, it results in a single equation similar to Eq. (9) that predicts both negative dissipation ( $\epsilon < 1$ ) and a frequency of  $\sim 0.04$  Hz, comparable with the numerically calculated frequency of  $\sim 0.035$  Hz reported in Ref. [23]. Our result suggest that, regardless of the microscopic parameters, the dynamic response of paced cells should scale with the ratio of the mesoscopic parameters (amplitude, frequency). Indeed, in Ref. [34] cardiac cells that were paced mechanically (with amplitude  $a \sim a_c$ ) were reported to entrain to the frequency of the probe up to frequency ratios  $\omega_p < 2.5$ . Above this threshold, beating switched to a combination of the frequencies of the cell and the probe. In the context of our theory, this corresponds to a crossing of the curve in Fig. 2 from the fully entrained to the nonentrained regime. In Fig. 2, we also reproduce the experimental data of Ref. [34] for entrained cells, where we fit the measured, experimental transition point at  $\omega_p \approx 2.5$  to the corresponding theoretical amplitude ratio  $a_p/a_c \approx 3.6$  obtained from the numerical solution of the paced Eq. (9) (consistent with the reported protocol of the experiment).

We would like to thank S. Tzlil, I. Nitsan, M. Lenz, D. Deviri, S. K. Nandi, N. Gov, A. Bernheim, and B. M. Friedrich for useful discussions. This work was funded by the U.S.-Israel Binational Science Foundation, the Israel Science Foundation, the Villalon Family Foundation, and the Perlman Family Foundation.

\*Corresponding author.

ohad.cohen@weizmann.ac.il

- [1] D. Bers, *Excitation-Contraction Coupling and Cardiac Contractile Force* (Springer Science & Business Media, Dordrecht, 2001), Vol. 237.
- [2] H.-T. Yang, D. Tweedie, S. Wang, A. Guia, T. Vinogradova, K. Bogdanov, P. D. Allen, M. D. Stern, E. G. Lakatta, and K. R. Boheler, *Proc. Natl. Acad. Sci. U.S.A.* **99**, 9225 (2002).
- [3] I. Kehat, D. Kenyagin-Karsenti, M. Snir, H. Segev, M. Amit, A. Gepstein, E. Livne, O. Binah, J. Itskovitz-Eldor, and L. Gepstein, *J. Clin. Invest.* **108**, 407 (2001).
- [4] S. Majkut, T. Idema, J. Swift, C. Krieger, A. Liu, and D. E. Discher, *Curr. Biol.* **23**, 2434 (2013).
- [5] D. M. Bers, *Nature (London)* **415**, 198 (2002).
- [6] D. Eisner, H. Choi, M. Diaz, S. Oneill, and A. Trafford, *Circ. Res.* **87**, 1087 (2000).
- [7] A. Reed, P. Kohl, and R. Peyronnet, *Global Cardiol. Sci. Pract.* **19** (2014).
- [8] M. Ibrahim, J. Gorelik, M. H. Yacoub, and C. M. Terracciano, *Proc. R. Soc. B* **278**, 2714 (2011).
- [9] H. H. Valdivia, J. H. Kaplan, G. Ellis-Davies, and W. J. Lederer, *Science* **267**, 1997 (1995).
- [10] N. J. Severs, *BioEssays* **22**, 188 (2000).
- [11] P. Martin and A. Hudspeth, *Proc. Natl. Acad. Sci. U.S.A.* **96**, 14306 (1999).
- [12] F. Jülicher, *C. R. Acad. Sci., Ser. Gen. Vie Sci.* **2**, 849 (2001).
- [13] F. Jülicher and J. Prost, *Phys. Rev. Lett.* **78**, 4510 (1997).
- [14] Y. Roongthumskul, R. Shlomovitz, R. Bruinsma, and D. Bozovic, *Phys. Rev. Lett.* **110**, 148103 (2013).
- [15] P.-Y. Plaçais, M. Bolland, T. Guérin, J.-F. Joanny, and P. Martin, *Phys. Rev. Lett.* **103**, 158102 (2009).
- [16] C. J. Jou, K. W. Spitzer, and M. Tristani-Firouzi, *Cell. Physiol. Biochem.* **25**, 419 (2010).
- [17] A. Atri, J. Amundson, D. Clapham, and J. Sneyd, *Biophys. J.* **65**, 1727 (1993).
- [18] J. Keizer and L. Levine, *Biophys. J.* **71**, 3477 (1996).
- [19] M. S. Jafri, J. J. Rice, and R. L. Winslow, *Biophys. J.* **74**, 1149 (1998).
- [20] J. Sneyd, J. M. Han, L. Wang, J. Chen, X. Yang, A. Tanimura, M. J. Sanderson, V. Kirk, and D. I. Yule, *Proc. Natl. Acad. Sci. U.S.A.* **114**, 1456 (2017).
- [21] Y. Tang and H. G. Othmer, *Biophys. J.* **67**, 2223 (1994).
- [22] G. Dupont, M. Berridge, and A. Goldbeter, *Cell Calcium* **12**, 73 (1991).
- [23] T. Höfer, *Biophys. J.* **77**, 1244 (1999).
- [24] R. Wilders, H. Jongsma, and A. Van Ginneken, *Biophys. J.* **60**, 1202 (1991).
- [25] M. Fill and D. Gillespie, *Biophys. J.* **115**, 1160 (2018).
- [26] See Supplemental Material at <http://link.aps.org/supplemental/10.1103/PhysRevLett.122.198101> for full derivation of our model for spontaneous oscillations, of the condition for entrained oscillations and for an example application of our method to a numerically solved model by Höfer.
- [27] G. Meissner, *J. Gen. Physiol.* **149**, 1065 (2017).
- [28] M. Doi and S. F. Edwards, *The Theory of Polymer Dynamics* (Oxford University Press, Oxford, 1988).
- [29] J. Yuval and S. A. Safran, *Phys. Rev. E* **87**, 042703 (2013).
- [30] O. Cohen and S. A. Safran, *Soft Matter* **12**, 6088 (2016).
- [31] P. Beek and W. Beek, *Human Movement Science* **7**, 301 (1988).
- [32] J. C. Sprott, *Elegant Chaos: Algebraically Simple Chaotic Flows* (World Scientific, Singapore, 2010).
- [33] X. Tang, P. Bajaj, R. Bashir, and T. A. Saif, *Soft Matter* **7**, 6151 (2011).
- [34] I. Nitsan, S. Drori, Y. E. Lewis, S. Cohen, and S. Tzlil, *Nat. Phys.* **12**, 472 (2016).
- [35] O. Cohen and S. A. Safran, *Sci. Rep.* **8**, 2237 (2018).
- [36] Y. Xia, J. B. McMillin, A. Lewis, M. Moore, W. G. Zhu, R. S. Williams, and R. E. Kellems, *J. Biol. Chem.* **275**, 1855 (2000).
- [37] E. Serena, E. Figallo, N. Tandon, C. Cannizzaro, S. Gerecht, N. Elvassore, and G. Vunjak-Novakovic, *Exp. Cell Res.* **315**, 3611 (2009).
- [38] M. Radisic, H. Park, H. Shing, T. Consi, F. J. Schoen, R. Langer, L. E. Freed, and G. Vunjak-Novakovic, *Proc. Natl. Acad. Sci. U.S.A.* **101**, 18129 (2004).
- [39] O. Scheel, S. Frech, B. Amuzescu, J. Eisfeld, K.-H. Lin, and T. Knott, *Assay Drug Devel. Technol.* **12**, 457 (2014).

- [40] H.-J. Berger, S. K. Prasad, A. Davidoff, D. Pimental, O. Ellingsen, J. Marsh, T. Smith, and R. Kelly, *Am. J. Physiol. Heart Circ. Physiol.* **266**, H341 (1994).
- [41] A. K. Peter, H. Cheng, R. S. Ross, K. U. Knowlton, and J. Chen, *Prog. Pediatr. Cardiol.* **31**, 83 (2011).
- [42] H. Hu and F. Sachs, *J. Mol. Cell. Cardiol.* **29**, 1511 (1997).
- [43] P. Hanggi and P. Riseborough, *Am. J. Phys.* **51**, 347 (1983).
- [44] R. Adler, *Proc. IRE* **34**, 351 (1946).